

SANDIA REPORT

SAND2014-18776

Unlimited Release

Oct 2014

Liquid Hydrogen Release and Behavior Modeling: State-of-the-Art Knowledge Gaps and Research Needs for Refueling Infrastructure Safety

Isaac W. Ekoto¹, Ethan Hecht¹, Chris San Marchi¹, Katrina M. Groth¹, A. Christine LaFleur¹, Nitin Natesan², and Michael Ciotti² and Aaron Harris³,

¹Sandia National Laboratories

²Linde LLC

³Air Liquide Corporation

Prepared by
Sandia National Laboratories
Albuquerque, New Mexico 87185 and Livermore, California 94550

Sandia National Laboratories is a multi-program laboratory managed and operated by Sandia Corporation, a wholly owned subsidiary of Lockheed Martin Corporation, for the U.S. Department of Energy's National Nuclear Security Administration under contract DE-AC04-94AL85000.

Approved for public release; further dissemination unlimited.



Sandia National Laboratories

Issued by Sandia National Laboratories, operated for the United States Department of Energy by Sandia Corporation.

NOTICE: This report was prepared as an account of work sponsored by an agency of the United States Government. Neither the United States Government, nor any agency thereof, nor any of their employees, nor any of their contractors, subcontractors, or their employees, make any warranty, express or implied, or assume any legal liability or responsibility for the accuracy, completeness, or usefulness of any information, apparatus, product, or process disclosed, or represent that its use would not infringe privately owned rights. Reference herein to any specific commercial product, process, or service by trade name, trademark, manufacturer, or otherwise, does not necessarily constitute or imply its endorsement, recommendation, or favoring by the United States Government, any agency thereof, or any of their contractors or subcontractors. The views and opinions expressed herein do not necessarily state or reflect those of the United States Government, any agency thereof, or any of their contractors.

Printed in the United States of America. This report has been reproduced directly from the best available copy.

Available to DOE and DOE contractors from

U.S. Department of Energy
Office of Scientific and Technical Information
P.O. Box 62
Oak Ridge, TN 37831

Telephone: (865) 576-8401
Facsimile: (865) 576-5728
E-Mail: reports@adonis.osti.gov
Online ordering: <http://www.osti.gov/bridge>

Available to the public from

U.S. Department of Commerce
National Technical Information Service
5285 Port Royal Rd.
Springfield, VA 22161

Telephone: (800) 553-6847
Facsimile: (703) 605-6900
E-Mail: orders@ntis.fedworld.gov
Online order: <http://www.ntis.gov/help/ordermethods.asp?loc=7-4-0#online>



SAND2014-18776
Unlimited Release
Oct 2014

Liquid Hydrogen Release Risk and Behavior Modeling: State-of-the-Art, Knowledge Gaps, and Research Needs for Refueling Infrastructure Safety

Isaac W. Ekoto and Ethan Hecht
Hydrogen and Combustion Technologies
Sandia National Laboratories
7011 East Avenue, MS 9052
Livermore, CA 94550

Chris San Marchi
Hydrogen & Metallurgy Science
Sandia National Laboratories
7011 East Avenue, MS 9161
Livermore, CA 94550

Katrina M. Groth and A. Christine LaFleur
Risk and Reliability Analysis
Sandia National Laboratories
P.O. Box 5800, MS 0748
Albuquerque, NM 87185

Nitin Natesan
Linde LLC
2389 Lincoln Avenue, Hayward, CA 94545
Hayward, CA

Mike Ciotti
Linde LLC
575 Mountain Avenue
Murray Hill, NJ 07974

Aaron Harris
Air Liquide Corporation
2700 Post Oak Blvd.
Houston, TX 77056

Executive Summary

As demand for hydrogen fuel increases with the introduction of fuel cell electric vehicles (FCEV), there will be increased pressure to minimize fueling station footprints and lower costs while maintaining safety and performance. The DOE Energy Efficiency and Renewable Energy Fuel Cell Technology Office (EERE FCTO) supports the initial build-out of hydrogen fueling stations through the development of tools needed to implement a risk-informed approach to station design and siting. Transformational EERE investments have previously supported the successful implementation of fire safety codes for compressed gaseous hydrogen systems (e.g., NFPA 55 and 2) using a risk-informed approach.

Bulk liquid hydrogen storage has the benefit of a higher storage potential that enables greater station throughput over similarly sized gaseous systems. However, data for model development and validation of liquid hydrogen releases — critical information needed for risk-based strategies — is unavailable due to a lack of adequate science-based test platforms with full control over release boundary conditions. Accordingly, current prescriptive liquid hydrogen bulk-storage separation distances are based on subjective expert opinion, and may be overly-conservative relative to similar bulk gaseous hydrogen storage system requirements. In practice, current liquid hydrogen separation distances have become a major impediment to fueling station deployments.

This work summarizes the current scientific consensus and knowledge gaps regarding cryogenic releases. Quantitative risk assessment (QRA) is presented as a means of informing fire safety codes, underscoring the need for validated, reduced-order models as a backbone for this approach. A review of the data and detailed modeling of cryogenic releases in the scientific literature is presented, with a noticeable dearth of validated models, or appropriate data to validate these models. The state-of-the-art in reduced-order hydrogen behavior modeling is described, which is advanced for gaseous releases, but requires development for liquid releases. Challenges associated with modeling cryogenic hydrogen releases largely stem from the multi-phase flows and phase change behaviors encountered during these releases.

A reduced-order model that breaks stream-wise flow regimes for cryogenic releases into discrete zones is expected to capture the correct physics. Zones furthest from the release are expected to perform well where the jet has warmed to temperatures more characteristic of gaseous releases. However, in the zones near the release, complex thermodynamic state modeling and multi-phase flows require assumed models for relevant behavior, that have not yet been properly validated.

Finally, this work describes a new capability being developed for controlled cryogenic hydrogen releases that can be used to improve and validate deterministic liquid hydrogen release models. The basic approach will follow a template used previously to characterize high-pressure gaseous hydrogen releases. The concept is to integrate a novel dual-stage heat-exchanger into the existing Turbulent Combustion Laboratory infrastructure to reduce supply gaseous hydrogen flows to the desired temperature — potentially creating mixed-phase flows — with the hydrogen exiting through a custom nozzle. High-fidelity Rayleigh scatter imaging diagnostics will be used to measure relevant release phenomena. Data developed from this effort will advance the creation of release models for low-temperature hydrogen leaks, which will enable risk-informed approaches to liquid hydrogen bulk storage safety.

Acknowledgments

The authors gratefully acknowledge the many productive discussions with the various stakeholders. These include but are not limited to Jennifer Yan and Ronald Lee from Linde LLC for engineering design support for lab upgrades, Gary Hux and Kent Robbins from Sandia for assistance with safety related issues pertaining to the use of liquid hydrogen as a coolant gas, Bill Houf and Bill Winters from Sandia (retired) for productive discussions regarding modeling issues, and the DOE FCTO Safety Codes and Standards program manager Will James for organizational support.

Contents

1	Introduction.....	11
1.1	Background.....	12
1.2	Quantitative Risk Assessment.....	12
1.3	Review of Liquid Hydrogen Experiments and Modeling.....	15
1.4	Approaches to Reduced-Order Hydrogen Release and Hazard Modeling	17
1.5	Gaps Identified.....	20
2	COLDPLUME Model Description.....	23
2.1	Zone 0 – zone of accelerating flow.....	24
2.2	Zone 1 – zone of underexpanded flow.....	25
2.3	Zone 2 – zone of initial entrainment and heating	26
2.4	Zones 3 and 4 – developing and fully developed flow zones	27
3	Proposed Experimental Approach to Model Validation.....	29
4	Summary and Recommendations	33
	References.....	35
	Distribution	45

Figures

Figure 1: Process flow diagram of the hydrogen-specific QRA approach used in codes and standards revision. Boxes highlighted in white denote areas determined by QRA models, boxes in dark gray are explicitly calculated via physics informed behavior models, and boxes in light-gray are for areas that accept both incident- and behavior-informed risk modeling. 13

Figure 2: Conceptual one-dimensional liquid hydrogen leak model (taken from Houf and Winters [67])..... 23

Figure 3. Schematic layout of the proposed Sandia/CA Cryogenic Hydrogen Release Laboratory that illustrates the two-state heat-exchanger (liquid nitrogen and liquid hydrogen) to rapidly cool supplied gaseous hydrogen to the desired cryogenic temperature at the nozzle exit..... 29

Tables

Table 1. Amount of liquid nitrogen coolant required for the 1st stage heat-exchanger and either liquid hydrogen or liquid helium coolant required for the 2nd stage heat-exchanger hydrogen flow rates between 100 and 1000 SLPM. The hydrogen inflows are at 10 bar atmospheric, and the exit temperature are either 35 K (cold vapor) or 31.3 K saturated liquid..... 30

Nomenclature

AHJ	Authority Having Jurisdiction
ALARP	As Low As Reasonably Possible
BAM	Battelle Ingenieurtechnik
BLEVE	Boiling Liquid Expanding Vapor Explosion
BST	Baker–Strehlow–Tang
CFD	Computational Fluid Dynamics
DOE	Department of Energy
EERE	Energy Efficiency and Renewable Energy
FCEV	Fuel Cell Electric Vehicle
FCTO	Fuel Cell Technology Office
FRA	Fire Risk Assessment
HDE	Homogeneous Direct Evaluation
HSL	Health and Safety Laboratory
HyRAM	Hydrogen Risk Assessment Model
ICESAFE	Integrated Cable Energy Safety Analysis Facility and Equipment
ISO	International Standards Organization
LFL	Lower Flammability Limit
LH2	Liquid Hydrogen
LHe	Liquid Helium
LN2	Liquid Nitrogen
ME	Multienergy
NASA	National Aeronautics and Space Administration
NFPA	National Fire Protection Agency
NIST	National Institute of Science and Technology
OEM	Original Equipment Manufacturer
QRA	Quantitative Risk Assessment
SAFETI	Software for the Assessment of Flammable, Explosive and Toxic Impact
SDO	Standards Development Organization
SLPM	Standard Liters Per Minute
SNL	Sandia National Laboratories
TNO	Netherlands Organization for Applied Scientific Research (Toegepast Natuurwetenschappelijk Onderzoek)

1 Introduction

Widespread hydrogen use as an alternative fuel for vehicles will require significant infrastructure upgrades to accommodate increased bulk transport, storage, and delivery. Brown et al. [1] performed a detailed economic analysis to assess potential fuel cell electric vehicle (FCEV) deployment rates in a proposed network of 68 hydrogen refueling stations clustered in urban areas throughout the state of California. They found such a network could rapidly drive FCEV fueling costs below that of equivalent gasoline vehicles and that both compressed gaseous and liquid delivery station technologies would be profitable long-term even with relatively low FCEV deployment rates. They further noted that despite higher bulk liquid storage system capital costs, the return on investment was 50–75% greater relative to compressed gas storage due to the higher station throughput enabled by larger liquid system storage densities. However, Harris [2] pointed out that it is doubtful that more than a handful of prospective station sites could meet current prescriptive safety guidelines for bulk liquid hydrogen storage from chapter 8 of the 2011 edition National Fire Protection Agency Hydrogen Technologies Code (NFPA 2 [3]). Liquid hydrogen bulk storage separation distances from NFPA 2 for lot lines, building openings or air intakes are in some cases more than twice as large as similar bulk gaseous storage systems; requirements that are prohibitive for space-constrained sites (typical in urban and suburban markets). Moreover, even for gaseous hydrogen storage there is not uniform separation distance requirements for different countries, since these values may be offset by other more restrictive system requirements [4]. The ISO Technical Committee 197 is currently working to standardize pan-European separation distances in addition to other relevant system safety requirements. It is also important to note that current prescriptive liquid hydrogen bulk-storage separation distances are based largely on subjective expert opinion rather than physical models, and thus may be overly-conservative (i.e., excessively large).

Codes and standards development that governs bulk storage and transport of liquid hydrogen, particularly for retail fuel station environments, requires a thorough understanding of release and dispersion characteristics over a range of realistic scenarios and environmental conditions. The desire to site large hydrogen quantities for FCEV fueling infrastructure drives the interest in placing bulk flammable cryogen storage at fueling facilities in urban and suburban areas. This storage requirement contrasts with traditional industrial uses of flammable cryogens that are not as space-constrained and can accommodate large safety separation distances. It is also important to consider specific activities such as setback distances where fuel transfer connections are made or broken.

Most releases are expected to be highly turbulent and heavily influenced by buoyancy, with dispersion affected by: flashing, multi-phase flows, heat transfer, pool formation, ambient conditions (e.g., temperature, humidity, wind), ground effects, and obstacles/barriers. Extreme cold temperatures can also condense or even freeze ambient air during spills, which differentiates these releases from those of liquid natural gas and can result in unique hazards that likewise need to be understood. At present, available experimental data in the literature is scant. The data that does exist is generally of insufficient quality for model development/validation due to poor boundary condition control and/or low measurement fidelity. This lack of high-quality data has accordingly meant that detailed multidimensional simulations and analytic models have achieved limited capability or have not been properly validated. Controlled experiments with high-fidelity

diagnostics are needed to generate parametric databases that can be leveraged for model development and validation.

1.1 Background

Lots in urban and suburban areas that are desirable for siting hydrogen refueling stations are almost uniformly too small to meet prescriptive separation distance requirements from chapter 8 of NFPA 2 when hydrogen is stored as a cryogen. Similar separation distance requirements for gaseous hydrogen stations were reduced by use of a risk-informed process [5] through the use of Quantitative Risk Assessment (QRA) in conjunction with underlying physical models that provide a defensible and traceable basis for separation distances. A similar process is envisioned for liquid hydrogen storage in future revisions to NFPA 2. Prescriptive separation distances for bulk liquid hydrogen systems — those larger than 150 L (39.7 gallons) [3] — will be evaluated in terms of risk and in concert with various mitigation controls required in the code.

To add flexibility to the siting process, a performance-based certification chapter has also been included in NFPA 2 (chapter 5). For performance-based certification, the station operator must demonstrate that an acceptable level of system safety has been achieved relative to the prescriptive requirements. Such an approach requires the use defensible QRA tools to establish and quantify risk scenarios, potential losses, mitigation measures, relevant physical processes, and inherent uncertainties. Hazard mitigation measures that may be appropriate to further reduce separation distances include barriers [6], sensors [7-9], or some combination of system isolation and flow restriction [10]. At the moment, physics-informed QRA tools have not been developed for refueling infrastructure applications. A range of tools exist to conduct QRA for oil and gas applications (e.g., SAFETI, RiskSpectrum), however, these tools lack validated models for hydrogen behavior in the parameter ranges relevant to fueling infrastructure [11]. Ongoing efforts to develop such a tool have made progress integrating gaseous hydrogen behavior models [12, 13], although liquid hydrogen behavior models remain a major gap [14].

1.2 Quantitative Risk Assessment

Quantitative Risk Assessment has long been used to provide a defensible scientific foundation for safety analyses in the nuclear power, oil and gas, and aviation and aerospace industries. QRA assigns the probability of different user identified consequences through the use of models encoded with background and statistical information to provide a reasoning framework for multiple decision options. In essence, QRA builds a bridge between scientific knowledge (e.g., experiments, theoretical models), engineering data, industry practices, and decision makers (e.g., codes and standards organizations).

For codes and standards, QRA provides a framework to establish a common understanding of the system safety level (based on robust science and engineering models) and then leverage that basis to make transparent safety decisions. The NFPA developed a guidance document to clarify when and how to apply QRA¹ for codes and standards development [15], but does not prescribe

¹ The NFPA guide refers to Fire Risk Assessment (FRA). To eliminate confusion and maintain consistency with other industries, we use the term QRA in lieu of FRA in this report.

a particular analysis method or criteria. Typical consequence metrics include: fatalities, injuries, economic losses, environmental or property damage, cultural or reputation loss, and business interruption. Acceptance criteria are established through close interactions with stakeholders and funding bodies, along with detailed surveys of existing risk benchmarks.

An overview of the QRA process defined for hydrogen systems is shown in the flow diagram in Figure 1. For gaseous hydrogen systems, the primary physical effects are the radiative heat flux from a jet-flame or the substantial overpressure from a delayed ignition event [16]. The process was originally defined by Groth et al. [17], and is similar to the process used by LaChance et al. [5] to establish NFPA 2 separation distances for gaseous hydrogen. The approach is also being implemented in the Hydrogen Risk Assessment Model (HyRAM) under development by Sandia to support additional revisions to hydrogen codes and standards [12].

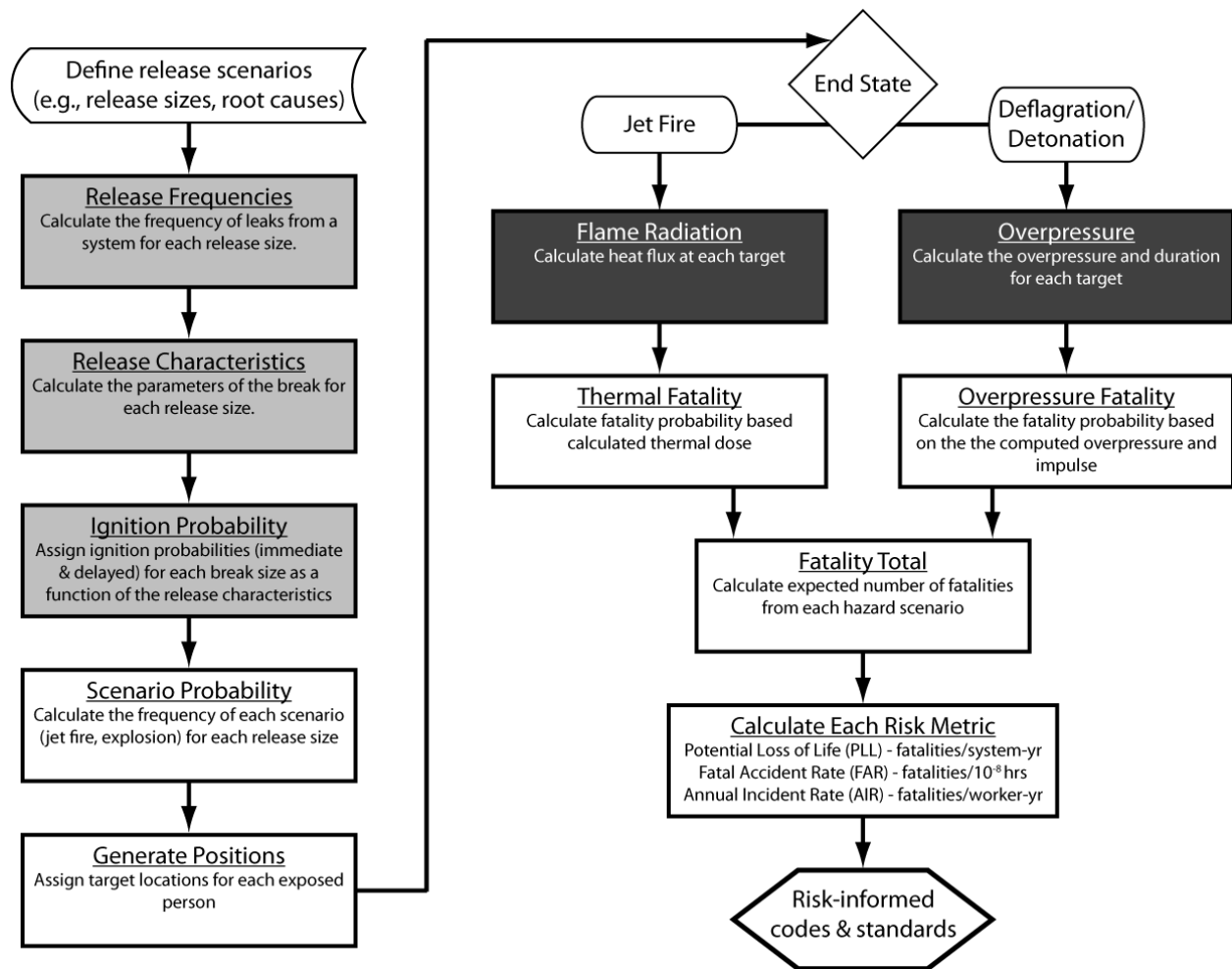


Figure 1: Process flow diagram of the hydrogen-specific QRA approach used in codes and standards revision. Boxes highlighted in white denote areas determined by QRA models, boxes in dark gray are explicitly calculated via physics informed behavior models, and boxes in light-gray are for areas that accept both incident- and behavior-informed risk modeling.

Figure 1 shows how a combination of scientific and statistical models, component performance data, and system information are used to define and quantify risk scenario information (at the

start of the flow chart). Common accident sequence initiating events can come from incident databases (e.g., H2Incidents.org [18] or the Hydrogen Incident and Accident Database [19]) or from risk models in similar industries and facilities. These events include component leaks, shutdown failures, or ruptures, with additional consideration given to human induced failure events [20]. In Figure 1, boxes highlighted in white denote decision states that are informed by a combination of logic and statistical models, along with relevant situational data. Decision state boxes in dark gray are explicitly calculated via physics-informed behavior models. Finally, decision state boxes in light-gray denote areas where relevant information can be derived from both statistical- and behavior-informed models. For more mature industries such as natural gas, these decision states would rely heavily on widely available operational data. However, the scarcity of hydrogen infrastructure reliability data due to relatively low numbers of hydrogen fueling stations worldwide necessitates the behavior-informed approach described above.

While behavior models exist for natural gas and other flammable gases, differences in the systems (e.g., storage pressures, storage temperatures, material compatibility), operating conditions, and physical characteristics (e.g., diffusion rates, flammability limits, flame speeds, heating value) limit model applicability to hydrogen systems. These core differences also limit the applicability of commercial software packages such as PHAST and SAFETI. A further consideration is the unacceptably high uncertainty in calculated risk results due to the lack of reliability data cited above. For example, model values for hydrogen or syngas jet flame radiative heat flux values are under-predicted by 40% or more in the near-field (distances within half the visible flame length), while other critical parameters such as flame length and tilt are likewise poorly predicted [21-23].

Detailed physical models are needed to understand and characterize hydrogen behaviors relevant to most large-scale accident scenarios. It should be noted that while safety engineering nomograms are useful tools to identify immediate hazards, detailed behavior models are needed to identify complex physical interactions present in most large-scale accident scenarios. For example, there is a need to assess the impact of mitigation strategies beyond separation distances, such as the effect of strategic barrier wall use or identification of optimal layouts for system components and safety equipment (e.g., sensors, process isolation, flow restriction); something not easily accomplished with process safety charts. Importantly, the behavior models must be computationally efficient so that vast situational spaces can be efficiently evaluated; accordingly, detailed computational fluid dynamics simulations (CFD) would likewise be prohibitive. Thus, reduced-order behavior models that are capable of successfully capturing the characteristics of complex physical processes are a major need. Numerous examples where reduced order-codes have augmented risk analysis include the PHAST and SAFETI packages cited above for oil and gas applications along with the EPA developed ALOHA gaseous dispersion code and the SNL developed MELCOR code for nuclear power plant safety. However, because behavior models in these codes were in many instances not specifically developed for hydrogen, they do not have the capability to sufficiently model relevant hydrogen release and combustion phenomena. Accordingly, validated hydrogen behavior models form a critical piece of the framework for risk-informed hydrogen codes and standards.

1.3 Review of Liquid Hydrogen Experiments and Modeling

A comprehensive review of state-of-the art hydrogen system safety knowledge is given by Kotchourko et al. [24], which includes a detailed discussion of liquid hydrogen systems. Their findings along with additional relevant information are summarized in the following section. In their review, they note that Pritchard and Rattigan [25] identified “the consequences of an accidental spillage or leak of liquid hydrogen are poorly understood, particularly the initial stages of pool spread and vaporization.” The limited experimental data available in the scientific literature [26-35] is generally of insufficient quality for model development/validation due to poor control of the boundary conditions or low measurement fidelity. Accordingly, there is the risk that the use of improperly validated models to establish safety envelopes could be detrimental to the emergence of hydrogen as a transportation fuel.

Early safety related release experiments by NASA focused on hydrogen vapor cloud dispersion from large-scale liquid hydrogen spills [26, 27]. For these experiments, controlled ground-level spills from storage containers as large as 5.7 m³ (1500 gal) were performed over a roughly 35 s release test. Instrumented towers downwind of the spill site were used to record vapor cloud temperatures, hydrogen concentrations, and turbulence levels. For rapid spills, as would be expected from catastrophic containment vessel failures, thermal and momentum-induced turbulence was observed to quickly dissipate cloud concentrations to non-flammable levels. Nonetheless, a flammable cloud was found to hug the ground for up to 100 m downstream of the release. Complementary large-scale liquid release experiments (up to 650 L, or 170 gal in 60 s) that simulated spills in residential areas were performed by Battelle Ingenieurtechnik (BAM) [28], with pool spreading rates and gas-cloud concentrations measured at discrete locations. Like their NASA counterparts, BAM researchers concluded that ground heat transfer effects and fast dissipation rates helped limit the size and duration of LH2 pools and flammable clouds.

For simulations of the NASA experiment [26, 27], Sklavounos and Rigas [36] used the CFX commercial solver and Middha et al. [37] used the FLACS commercial solver. Both groups achieved a factor of 2 agreement with measured concentrations. However, it should be noted that the factor 2 agreement is not acceptable for hydrogen since the discrepancy will greatly affect overpressure calculations during delayed ignitions. Venetsanos and Bartzis [38] used the ADREA-HF code to investigate the sensitivity of select parameters for the same experiments, and found optimal agreement occurred when the cloud source was modeled as a two-phase jet instead of a pool. Remaining simulation and measurement discrepancies were attributed to unaccounted for changes in wind direction and speed, the absence of humidity in the model, and incorrect soil temperature predictions for ground heat flux models. An updated code was later used to simulate a LH2 hose break at a mock re-fueling station, with the effects of wind and the presence of obstacles systematically investigated [39]

An early effort to simulate the BAM spill experiments was performed by Schmidt et al. [40] using the commercial CFD package Fluent. The absence of suitable LH2 physics models forced the spill to be modeled as a gas-phase release using an estimated pool vaporization rate due to surface heat transfer. While model agreement to the data was somewhat satisfactory, they conclude that more experimental data of relevant phenomena, with careful control of the boundary conditions, is needed for conclusive model validation. In another approach, Statharas et al. [41] applied a simplified hydrogen vaporization process model with a constant hydrogen flow rate

and fixed liquid fraction, to initialize a simulation of cloud dispersion using the ADREA-HF CFD solver. By including ground heat transfer to the cloud, the agreement between experiments and simulations was significantly improved, although concentrations were still off by a factor of 2 in many regions.

More recently, 3 outdoor LH2 spill tests were performed by the United Kingdom Health and Safety Laboratory (HSL) [33, 34], which had a fixed 0.071 kg/s flow-rate from a 2.66 cm diameter release nozzle and release durations between 248 and 556 seconds. One release was vertically orientated, while the other two were positioned horizontally at different heights above the ground (860 mm vs. 3.4 mm) to examine the impact of surface heat-transfer and modified entrainment on dispersion characteristics. Ambient pressure, temperature, and humidity along with wind-speed and direction were monitored real time at multiple locations. Thermocouples measured gas-cloud temperatures at several locations downwind of the release, with hydrogen concentrations calculated under the assumption of adiabatic mixing with the ambient. Surface temperatures were also measured at discrete locations and depths around the release point to both calculate the extent of liquid pool formation and the amount of heat transfer to the release plume. During the release, a solid deposit was observed where the hydrogen impinged on the ground. The authors speculated that the deposit consisted of a potentially explosive mixture of frozen oxygen and nitrogen. Unlike the BAM and NASA tests, the HSL releases were subsequently ignited to evaluate the radiative and overpressure characteristics of liquid hydrogen flash fires. In some cases after ignition two distinct deflagration events were observed; one attributed to gas-phase cloud combustion and the other to a quasi-detonation of the oxygen-rich ground deposit.

In their CFD analysis of the HSL experiments [33, 34] with the FLACS code, Ichard et al. [42] performed a sensitivity study, where they increased the source term gas volumetric fraction from 0.76 to 1, with the best agreement to the data achieved with a 0.99 volumetric gas fraction. Jaekel et al. [43] performed a similar study using the CFX solver, and found the best agreement with the measurements occurred with a liquid mass fraction between 50% and 75%. Since the saturated liquid density is roughly 50 times greater than the corresponding saturation gas phase density, the two simulation results are in reasonably good agreement. Nonetheless, wall temperature distributions and pool front velocities were not well predicted. Giannissi et al. [44] simulated the HSL liquid hydrogens releases with the ADREA-HF code, with a systematic evaluation of the influence of ambient humidity, wind speed/direction, and two-phase slip modeling of condensed water on simulation results. They found that for humid air, condensed and frozen water particles assumed a velocity defect relative to the gas-phase flow that required appropriately tuned slip modeling. When slip velocities were accounted for, ice and water particles — along with possible condensed air constituents — fell to the ground, which resulted in a more buoyant hydrogen/air cloud that better agreed with the experimental measurements.

Friedrich et al. [35] performed release and combustion experiments for cryogenic hydrogen jets with release temperatures between 34 – 65 K and pressures from 0.7 – 3.5 MPa in the ICESAFE (Integrated Cable Energy Safety Analysis Facility and Equipment) facility located at the Karlsruhe Institute of Technology (KIT). Hydrogen concentration decay rate measurements preserved the linear dependence when plotted against a density-scaled release diameter. For ignited cryogenic hydrogen jets, the operation states for three possible flame modes were schematically mapped: 1) ignition flash-back to the release nozzle followed by a stable jet flame, 2) a stable lifted flame without flash-back, and 3) a transient burn with subsequent blow-off. For

the jet flames examined no overpressure or noise hazards were observed. Note that as of the writing of this report that no attempt to simulate the release characteristics has been performed.

1.4 Approaches to Reduced-Order Hydrogen Release and Hazard Modeling

Effective reduced-order model development requires consideration of all accident scenario event sequences, with accurate physical behavior prediction at each step. Models must predict release and dispersion characteristics under a range of initial conditions, flame ignition and sustainment probability, and comprehensive quantification of jet flame and overpressure hazards. Moreover, the models must properly account for mitigation measures such as the use of barrier walls to shield from radiative heat fluxes or the use of explosion proof electrical equipment to lower ignition probabilities. Finally, it is crucial that the models work seamlessly with each other.

One efficient method of modeling the complex flow system of a hydrogen refueling station is a network flow model — where fluid flow is analogous to electrical network current flow, with pressure corresponding to voltage potential and resistance similar to flow friction. Flow network problems are inherently difficult to solve since the “resistors” are nonlinear and the pressure field is often coupled to network states such as temperature. The Sandia developed NETFLOW code combines a control volume finite element technique with the Greyvensteyn and Laurie method to solve coupled pressure and flow rate equations [45]. Variables accounted for include flow transients, compressibility, hydraulic head-loss, flow expansion/contraction, and flows through pumps; compressors; or components with known pressure drop/flow rate relationships. Model accuracy depends on the ability of flow behavior to be captured by one-dimensional flow conservation equations and local correlations for wall friction, heat transfer, and pressure loss. At the moment, the compressible flow solver is unable to account for incompressible liquid and multi-phase flows expected in typical liquid hydrogen systems, but upgrades are planned to enable modeling these flows.

To model gas dispersion, a Sandia developed one-dimensional integral model that invokes self-similarity for radial variables and solves the centerline conservation equations has been created [46]. Entrainment coefficients, jet-spreading ratios, and correlations for radial mixing statistics were empirically determined from extensive concentration measurements of hydrogen gas jets [47-50]. Buoyancy and momentum driven leak regimes have been identified and accounted for using functions based on the local Froude number. Similar models for generic [51, 52] and hydrogen gas releases [53] have been developed by other groups with slightly modified treatment of flow entrainment, but nonetheless reproduce the release characteristics of expanded jets from a range of release conditions. For slot jets, Epstein and Fauke [54] have developed a top-hat jet model to that calculates total flammable cloud mass and volumes for gas or volatile liquid releases and seems to agree well with existing datasets. Methods to account for pressure dissipation from viscous, inertial, and expansion effects across releases from cracks with varying tortuosity have been developed for ideal fluids [55], but have not yet been implemented in these dispersion models.

For releases where exit backpressures relative to ambient are above a critical ratio, the flow becomes choked and an underexpanded jet with complex near-field shock structure forms at the

exit. A Mach disk that can be several factors larger than the original release diameter serves as the boundary between the upstream supersonic and downstream subsonic regions. Notional nozzle models have been developed to predict the effective jet diameter, velocity, and thermodynamic state downstream of the Mach disk. Each model conserves mass [56-58], with more complex versions successively considering momentum conservation [59-61] and entropy conservation across a normal shock [62] to reduce the number of assumed boundary conditions. Model effectiveness for hydrogen has been evaluated experimentally by Ruggles and Ekoto [50] and numerically by Papanikolaou et al. [63], with Ruggles and Ekoto noting the importance of accurate state modeling for the notional nozzle model formulations. A particular weakness for all models is the assumption of a homogenous effective release point (i.e., plug flow), even though detailed simulations [64, 65] and qualitative visualizations [50] suggest there are distinct inner core and outer slip regions that should be modeled separately. Work is ongoing to develop improved notional nozzle models and a set of validation data. It should be noted that work is likewise ongoing to investigate and develop models for non-circular (e.g., slot) releases [66-68].

Winters et al. [69-71] developed a homogeneous two-phase critical flow model for choked cryogenic hydrogen releases. A critical assumption was that multi-phase components were in thermal equilibrium. Travis et al. [72] subsequently updated the model, which they termed the homogeneous direct evaluation model (HDE), to allow for different temperatures of the multiphase components. The HDE model was validated against NASA cryogenic data for liquid and supercritical hydrogen, methane, nitrogen, and oxygen in terms of critical mass fluxes for a range of stagnation conditions [73, 74]. Li et al. used the PHAST software package to calculate harm-effect distances for LH2 [75] and cryo-compressed hydrogen [76] releases, with the HDE model used as the input boundary condition. However, the results were highly uncertain due to the simplified PHAST models and correlations that have not been validated for relevant hydrogen hazard phenomena (e.g., cold clouds, liquid pools, jet fires or fires, explosions).

Models that describe liquid hydrogen pool formation and spreading have been developed by several groups. Harstadt and Bellan [62] developed an analytical expression for minimum pool evaporation time based on hydrogen film-boiling rates. The LAUV computer code developed by Verfondern and Dienhart [30] uses an input integral jet model to describe pool formation, and is capable of modeling cryogenic liquid spreading and vaporization along either solid or water surfaces, with satisfactory agreement achieved between experiment data. Finally, Kim et al. [77, 78] applied a perturbation theory method to solve a physical model that describes LH2 pool spreading and found that their method was able to achieve nearly identical results to numerical solutions if third order perturbation solutions were considered.

For indoor hydrogen releases, the build-up and delayed ignition of flammable clouds can cause significant overpressure hazards. The severity of the resulting deflagration or detonation will depend on the local concentration and the extent of flammable accumulation; hence it is important to quantify the gas build-up characteristics. From large-scale fill-box experiments, buoyant gas releases into enclosures have been observed to form uniform accumulation layers at the ceiling [79-85]. Lowesmith et al. [80] developed a time-dependent gas buildup model for slow hydrogen/methane mixture releases. The model uses a 1D integral buoyant plume model to account for the source and the Kaye et al. fill-box model [84] to calculate the time-dependent layer thickness and concentration. The model further considers wind driven ventilation into and out of the enclosure, with the model results agreeing well with complementary measurements.

The two predominant methods to calculate overpressure and impulse from confined ignition of flammable mixtures are the Baker–Strehlow–Tang (BST) model and the multienergy (ME) model from the Netherlands based TNO organization [86, 87]. Source energy for both models is defined by either a spherical (BST) or hemispherical (ME) stoichiometric flammable cloud in a congested environment, with the dimensionless overpressure and positive impulse calculated as a function of energy-scaled distance. Note that the ME model scaled distance is defined from the cloud center location, while the distance from the congestion center is used for the BST model. Blast curve lookup tables in the BST model are generated from fractal based numerical models of vapor cloud flame front acceleration [88, 89], with blast strength proportional to the maximum cloud flame speed [90]. In contrast, the ME model uses empirically derived initial explosion strengths for vapor cloud flame front acceleration, with overpressure and impulse determined from a suite of blast charts as a function of scaled combustion energy [91]. For both approaches, computed overpressure and impulse values depend on the degree of fuel reactivity, confinement/obstruction, and distance available for flame acceleration [86, 92]. More recent BST models have developed correlations to account for enclosure ventilation [93-96], while newly developed time-dependent vent models [97] may be adapted to further improve predictions.

The BST and ME models have traditionally been considered for enclosures without stratified concentration layers. Bauwens and Dorofeev [98] developed an analytic overpressure model that describes the pressure increase from the adiabatic expansion due to the combustion of all flammable hydrogen/air mixtures within the enclosure (but neglecting local blast waves). Model performance was compared against hydrogen dispersion and ignition data from a scaled warehouse facility by Ekoto et al. [83], with the hydrogen release modeled by the open source CFD code, FireFoam. The agreement with the overpressure measurements was very good. Groth [99] later used a modified version of the Lowesmith et al. [80] gas layer model to simulate the hydrogen release and buildup within the scaled warehouse, and used these values to obtain the boundary conditions for the Bauwens and Dorofeev [98] analytic overpressure model. Scenario overpressure predictions were within 10% of the measured values using simplified models.

Whether a combustible hydrogen/air layer will lead to an explosive overpressure depends on the presence of an ignition source in the flammable region. For stratified mixtures of flammable gas and ambient and short duration ignition sources, it is further possible that given regions will be intermittently combustible as turbulence and convection sweep flammable mixtures into and away from the ignition source. To account for this behavior, the Flammability Factor has been developed, which is a derived scalar represented by the integrated flammable gas mole fraction probability density function (PDF) bounded by the upper and lower flammability limits [100-103]. The PDF shape needs to be empirically determined from well-controlled experiments or detailed computational simulations of relevant scenarios. Flammability limits for hydrogen in air under a range of temperatures and levels of dilution (e.g., from steam) can be determined computationally using combustion chemistry simulation tools such as CHEMKIN. A final consideration is the determination of whether an incipient ignition kernel will transition into a sustained flame or will be extinguished. This is a complex problem where flame sustainment competes with locally lean concentration levels, heat loss, and convective strain rates. At the moment, reduced-order modeling to predict flame sustainment is poorly developed.

The final hazard considered in this review is hydrogen jet-flame radiant heat flux exposures and elevated temperatures, which can lead to potentially lethal burns and severe respiratory damage

[16]. Empirical reduced-order models are often used to determine hazard boundaries [21, 104-111] with relevant release conditions (e.g., nozzle diameter, flow rate, gas type) used to estimate flammable envelopes and the radiant fraction — defined as the amount of flame energy converted into escaping radiant energy. Schefer et al. [59] reported that like hydrocarbon flames, hydrogen flame radiant fractions exhibit a logarithmic dependence on flame residence time. However, the absence of CO₂ or soot in the product stream results in lower overall radiant fractions [112]. Based on these observations, Molina et al. [113] developed a unified expression that treats the flame as a blackbody emitter with the radiant fraction expressed a function of flame residence time, adiabatic flame temperature, and product species Plank's mean absorption. Radiant heat flux predictions derived from conventional single point source models [106, 111] have been found to severely underpredict near-field measurements. Model prediction can be substantially improved, however, if distributed multi-source models are used and corrections for reflective radiation are applied [23]. The exception is for downstream measurements, where recorded radiative heat flux values remain well below model predictions. In response, Ekoto et al. [114] developed a 1D flame integral model to predict flame centerline trajectories that allowed the source emitter placement to be optimized. The updated model gives predictions to within 3% of downstream radiative heat flux measurements from large-scale (up to 50 m long) hydrogen jet flames if appropriate source modeling is applied.

1.5 Gaps Identified

Several research and modeling gaps exist for releases from liquid hydrogen storage systems. There is a clear need to adapt existing network flow models for cryogenic flows so that accurate release boundary conditions can be determined. Such an upgrade requires appropriate state modeling for incompressible liquid hydrogen flows along with multi-phase flows of liquids, non-ideal gases, and supercritical fluids. Additional requirements include updated methods to account for wall heat transfer and viscosity, flows through contractions and expansions, and non-equilibrium temperature effects that can impact mass flow rates. Experiments and numerical simulations will likely be needed to generate hydrogen specific datasets at relevant conditions.

Phase modeling has been observed to be a critical characteristic needed to accurately simulate liquid hydrogen dispersion behavior. However, to date there has been no effort to develop reduced-order modeling strategies for multiphase jet and plume flows that appropriately account for phase-velocity defects. Reduced-order wind modeling is likewise needed along with ground and solar heat transfer considerations. It should be further noted that while current gaseous flow dispersion models have been adapted to model liquid hydrogen flows, there is not yet sufficient experimental data to validate the developed modeling strategies. For example, initial entrainment rates and jet-spreading ratios have been adapted from gas jets, without any confirming data to suggest whether these assumptions are valid. Accordingly, in addition to overly cool gas-phase jets, data from initial liquid states are required for comprehensive plume modeling. High-resolution scalar concentration experiment data from well-controlled laboratory release jets that have varying levels of ambient humidity are also needed to develop/validate accurate multiphase slip models. Numerical simulations of the jet release experiments would be relied on to provide complementary data that otherwise are not measurable (e.g., liquid volume fractions).

Finally, the reduced-order models need to be able to accurately capture the dynamics of surface impingement and subsequent pool formation if needed. Barrier walls have long been considered

an effective consequence mitigation strategy for gaseous releases, and similar data is needed to show the effectiveness of these walls for liquid hydrogen releases. The most promising pathway is to incorporate the proper liquid hydrogen flow physics and thermodynamics into wall impingement models that take advantage of similarity jet spreading [115-118]. It is critical that these models are able to suitably predict the possibility of the formation of explosive solid oxygen deposits, since this represents an extreme hazard that has the capability to result in catastrophic consequences. Although these experiments would preferably be conducted within well controlled lab environments, safety considerations will likely force these experiments to remote test sites. Validated multidimensional modeling would play a critical role in verifying the performance of any developed reduced-order models.

2 COLDPLUME Model Description

The present section details a Sandia developed cryogenic hydrogen integral jet and plume model, COLDPLUME [46, 69-71], which is conceptually shown in in Figure 2. The model has subsequently been updated for choked flows with the HDE non-equilibrium, two-phase, single-component, critical (choked) flow model for cryogenic fluids originally developed by Travis et al. [72] to more accurately capture multi-phase behavior at the release plane. COLDPLUME is used to predict release characteristics from various real-world hydrogen storage states. Network flow models needed to account for internal system flows from the storage vessel to the release plane are not considered here; work is ongoing to update the Sandia developed NETFLOW code [45] to be suitable for liquid and multiphase cryogen flows and will not be discussed further here.

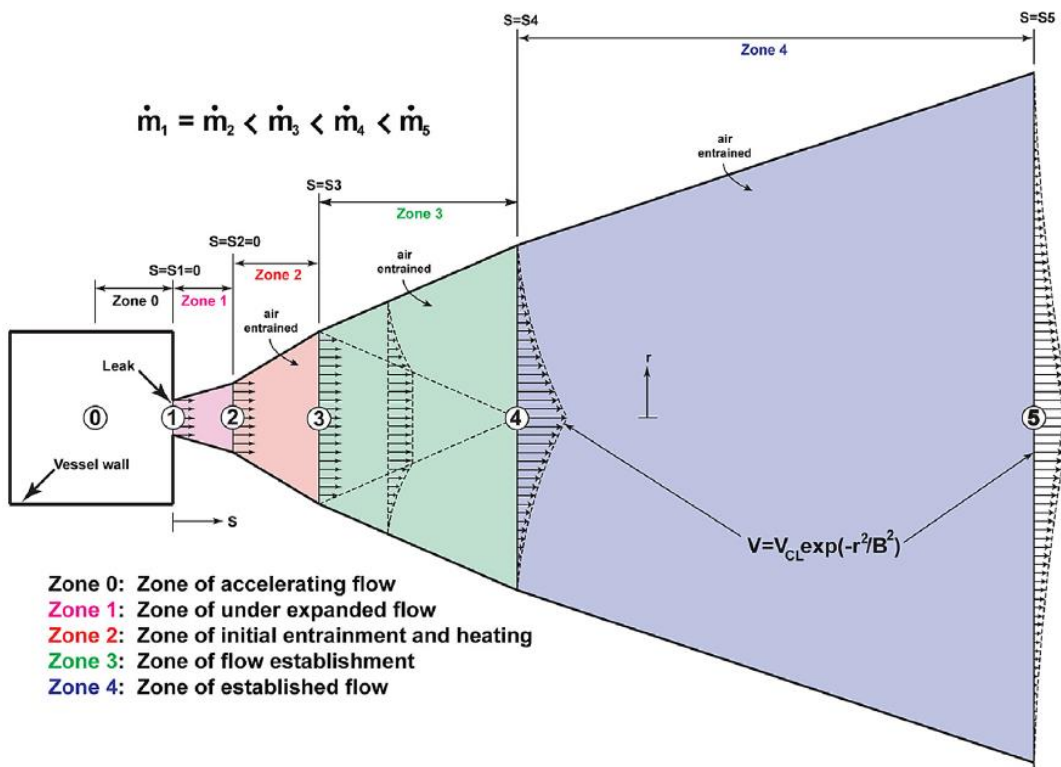


Figure 2: Conceptual one-dimensional liquid hydrogen leak model (taken from Houf and Winters [67]).

COLDPLUME divides the leak stream into a series of sequential Zones separated by discrete flow Stations where appropriate physics are captured, as shown in Figure 2. Note that the schematic is not drawn to scale, with Zones 0 – 3 considerably smaller than the final established flow zone (Zone 4). Upstream of Station 3, complicated thermodynamics require real gas state equations to account for multi-phase (liquid, vapor and possible solid phases) and non-ideal behavior for hydrogen-air mixtures. REFPROP [119], a program that utilizes thermodynamic models developed at the National Institute of Science and Technology (NIST), is used for state model calculations in the upstream Zones. Downstream of Station 3 (i.e., Zones 3 and 4), the

plume is modeled as an ideal gas mixture at atmospheric pressure. In the following sections, modeling assumptions and equations are presented for each zone in the leak jet.

2.1 Zone 0 – zone of accelerating flow

A key assumption for the stagnation condition is that hydrogen is stored as a pure substance in either a saturated vapor, saturated liquid, sub-cooled liquid, or superheated vapor state. It is further assumed that the leak area is open to the atmosphere and that all heat transfer, pressure drop, and potential energy changes due to the system flow have been captured prior to zone 0 (e.g., using a network flow code), with further changes considered negligible between the Stations 0 and 1. Additional assumptions are as follows:

- Multi-phase components have equal phase velocities.
- For vapors at saturation, liquids can be superheated; otherwise, the maximum liquid superheat is limited to the saturation temperature.
- Multi-phase components are isobaric.

The thermodynamic state at Station 0 is further assumed to have a small velocity just after the leak plane. The energy equation and the observation that flow acceleration to the leak plane is isentropic are used to determine Station 1 state variables and hydrogen mass flow rates.

$$\text{Eq. 1.} \quad w_1^2 = 2(h_0 - h_1)$$

$$\text{Eq. 2.} \quad s_1 = s_0$$

Here, w is the sound speed, while h and s are the specific enthalpy and entropy respectively. If the phase from Station 0 to Station 1 is constant, then no further modeling is required. For multi-phase flows, the HDE method initially assumes an isentropic flow expansion from the stagnation plane to the liquid saturation line, and later to the two-phase coexistence region. For general pure substances, the two-phase relationship between fluid properties and the quality, Q , are.

$$\text{Eq. 3.} \quad s = Q \cdot s_V + (1 - Q) \cdot s_L$$

$$\text{Eq. 4.} \quad v = Q \cdot v_V + (1 - Q) \cdot v_L$$

$$\text{Eq. 5.} \quad h = Q \cdot h_V + (1 - Q) \cdot h_L$$

where v is the specific volume. Subscripts V and L respectively denote pure fluids in the vapor or liquid phase. Accordingly, the two-phase sound speed can be expressed as:

$$\text{Eq. 6.} \quad w_1^2 = \left(\frac{\partial p}{\partial \rho_1} \right)_s = \frac{v_1^2}{\left(\frac{\partial v_1}{\partial p} \right)_s} = \frac{v_1^2}{Q \left(\frac{\partial v_L}{\partial p} \right)_s + (1-Q) \left(\frac{\partial v_V}{\partial p} \right)_s - (v_V - v_L) \left(\frac{\partial Q}{\partial p} \right)_s} =$$

$$\frac{v_1^2}{\frac{Q}{(\rho_V w_V)^2} + \frac{(1-Q)}{(\rho_L w_L)^2} - (v_V - v_L) \left(\frac{\partial Q}{\partial p} \right)_s}$$

The quality derivative with respect to pressure for constant system entropy uses Eq 3 to produce:

$$\text{Eq. 7.} \quad \left(\frac{\partial Q}{\partial p} \right)_s = \frac{-(s_V - s_L) \left(\frac{\partial s_L}{\partial p} \right)_{s_L} + (s_0 - s_L) \left[\left(\frac{\partial s_V}{\partial p} \right)_{s_V} - \left(\frac{\partial s_L}{\partial p} \right)_{s_L} \right]}{(s_V - s_L)^2}$$

It is assumed that s_V and s_L are respective functions of the vapor and liquid temperatures along with the constant pressure, which implies the respective isentropic pressure differentials are:

$$\text{Eq. 8.} \quad \left(\frac{\partial s_V}{\partial p}\right)_{s_V} = \left(\frac{\partial s_V}{\partial p}\right)_{T_V} \left(\frac{\partial p}{\partial p}\right)_{s_V} + \left(\frac{\partial s_V}{\partial T_V}\right)_p \left(\frac{\partial T_V}{\partial p}\right)_{s_V}$$

$$\text{Eq. 9.} \quad \left(\frac{\partial s_L}{\partial p}\right)_{s_L} = \left(\frac{\partial s_L}{\partial p}\right)_{T_L} \left(\frac{\partial p}{\partial p}\right)_{s_L} + \left(\frac{\partial s_L}{\partial T_L}\right)_p \left(\frac{\partial T_L}{\partial p}\right)_{s_L}$$

From Maxwell's fourth relationship, i.e., $\left(\frac{\partial s_L}{\partial p}\right)_T = -\left(\frac{\partial v}{\partial T}\right)_p$, and the definition of constant pressure specific heats, Eq. 8 can be rewritten as:

$$\text{Eq. 10.} \quad \left(\frac{\partial s_V}{\partial p}\right)_{s_V} = -\frac{\beta_V}{\rho_V} + \frac{c_{pV}}{T_V} \left(\frac{\partial T_V}{\partial p}\right)_{s_V} = -\frac{\beta_V}{\rho_V} + \frac{\left(\frac{c_{pV}}{T_V}\right)}{\left(\frac{dp_\sigma(T_V)}{dT_V}\right)}$$

Note that the parameters β and c_P are the volumetric expansivity and isobaric heat capacity respectively. If only properties at the saturation condition are considered, the liquid and vapor temperatures can be related by defining a "non-equilibrium" parameter, η , as:

$$\text{Eq. 11.} \quad \eta = \frac{T_s - T_V}{T_l - T_V}$$

Accordingly, Eq. 9 can be written as:

$$\text{Eq. 12.} \quad \left(\frac{\partial s_L}{\partial p}\right)_{s_L} = -\frac{\beta_L}{\rho_L} + \frac{c_{pL}}{T_L} \left(\frac{\partial T_L}{\partial p}\right)_{s_L} = -\frac{\beta_L}{\rho_L} + (1 - \eta) \frac{\left(\frac{c_{pL}}{T_L}\right)}{\left(\frac{dp_\sigma(T_V)}{dT_V}\right)}$$

REFPROP is called to calculate Station 1 liquid and vapor trial states.

Sound speed determination for liquid/vapor mixtures has been addressed extensively in the literature [120-122]. A relatively simple version by Chung et al. [123] and validated against bubbly two-phase flow data was used by Houf and Winters [71]. To compute the Station 1 state, the Station 1 pressure and entropy were initially set to the Station 0 values with pressure incrementally reduced by a small Δp . The Station 1 sound speed is then computed from REFPROP, with the velocity calculated from the energy equation (Eq. 1). If the velocity exceeds the sound speed, the flow is choked and a calculation exit condition is met. Alternatively, if the pressure is below atmospheric, the flow is unchoked and another exit condition is satisfied. Otherwise, p_1 is incrementally decreased until one of the exit conditions is met.

2.2 Zone 1 – zone of underexpanded flow

If the Station 1 flow is not choked, Zone 1 is ignored with the properties, flow area and velocity at Station 2 set to the corresponding Station 1 values. Otherwise, the underexpanded jet flow is modeled using one of the source models described in Section 1.4 to determine the conditions at Station 2. Our preferred source model is the variant by Yuceil and Ottugen [61], which was subsequently updated by the Abel-Noble equation of state [50]. Applying these assumptions yields the following conservation equations for Zone 1:

$$\text{Eq. 13.} \quad \dot{m}_1 = \dot{m}_2 = \rho_2 \left(\frac{\pi D_2^2}{4} \right) V_2$$

$$\text{Eq. 14.} \quad \left(\frac{\pi D_1^2}{4} \right) p_1 + \dot{m}_1 V_1 = \left(\frac{\pi D_2^2}{4} \right) p_{amb} + \dot{m}_1 V_2$$

$$\text{Eq. 15.} \quad h_1 + \frac{1}{2} V_1^2 = h_2 + \frac{1}{2} V_2^2$$

Determination of Station 2 source velocity, thermodynamic properties, and jet diameter is straightforward since the state and mass flow rate at Station 1 are known. Initially the Station 2 velocity and enthalpy are computed from Eqs. 14 and 15, with relevant thermodynamic variables computed from REFPROP. The Station 2 source diameter is then computed from Eq. 13. The Zone 1 length is assumed to be negligibly small compared to the downstream (on the order of 10 leak diameters or less for discharges for pressure ratios below ~ 10 [124]).

2.3 Zone 2 – zone of initial entrainment and heating

Zone 2 thermodynamics are complicated by the likely presence of multiphase mixtures with the phase components possibly not in mechanical or thermodynamic equilibrium. Moreover, an unknown amount of ambient air entrainment will likely condense or even freeze, which produces multi-component liquid phase mixtures that cannot be characterized by REFPROP. Accordingly, if the Zone 2 temperature exceeds the mixture gas phase temperature, Zone 2 can be neglected, with Station 2 properties transferred to Station 3. Otherwise, a “plug flow” turbulent entrainment model is invoked with the following assumptions:

- Air and hydrogen are simple compressible substances in mechanical/thermal equilibrium.
- The flow stream is turbulent and quasi-steady.
- Turbulent transport dominates molecular diffusion and only occurs at the jet periphery such that concentration, thermodynamic and concentration values are self-similar.
- Stream-wise turbulent diffusive transport is negligible compared to convective transport.
- Pressure is isobaric (i.e., atmospheric).
- Potential energy changes are negligible.
- Short zone lengths and large local Froude numbers mean Buoyancy is negligible.
- The Station 3 temperature is specified as the point where hydrogen/air mixtures at atmospheric pressure exist in the gas phase (currently 47 K for REFPROP).

Based on the above assumptions and mass conservation, the Station 3 mass flow rate is equal to the pure hydrogen inflow and any turbulently entrained air along the jet periphery. Since the zone is isobaric, net pressure forces on the zone are zero with constant momentum flux. Energy conservation considers the kinetic and chemical energy of both the hydrogen entering the zone and hydrogen/air mixture leaving the zone, as well as the energy contained in the entrained air. The resulting mass, momentum, and energy conservation equations for Zone 2 are:

$$\text{Eq. 16.} \quad \dot{m}_2 + \dot{m}_{air} = \dot{m}_3 = \rho_3 \left(\frac{\pi D_3^2}{4} \right) V_3$$

$$\text{Eq. 17.} \quad \dot{m}_2 V_2 = \dot{m}_3 V_3$$

$$\text{Eq. 18.} \quad \dot{m}_2 \left(h_2 + \frac{1}{2} V_2^2 \right) + \dot{m}_{air} h_{air} = \dot{m}_3 \left(h_3 + \frac{1}{2} V_3^2 \right)$$

Station 3 enthalpy is determined from the specified Station 3 temperature, atmospheric pressure, and Station 3 mixture composition through appropriate REFPROP calls. These conservation equations are solved iteratively, since air entrainment and zone exit conditions cannot be explicitly calculated *a priori*.

2.4 Zones 3 and 4 – developing and fully developed flow zones

Methods to model Zones 3 and 4 were originally developed by Gebhart et al. [125] and most recently used by Winters and Houf [70, 71]. The assumptions are similar to those given for Zone 2 except buoyancy and wind forces are now considered, and the flow is no longer a plug flow. Zone 3 is a relatively short zone where the leak jet transitions from plug flow to fully developed flow. Most discussion here relates to the fully developed flow zone, Zone 4, since this is by far the largest zone in the leak model. The governing conservation equations have the form:

$$\begin{aligned}
 \text{Eq. 19.} \quad & \frac{d}{ds} \int_0^\infty \rho V r dr = \frac{\rho_{amb} E}{2\pi} && \text{(continuity)} \\
 \text{Eq. 20.} \quad & \frac{d}{ds} \int_0^\infty \rho V^2 \cos \theta \cos \sigma r dr = \frac{F_D}{2\pi} \sqrt{1 - \cos^2 \theta \cos^2 \sigma} && \text{(x-momentum)} \\
 \text{Eq. 21.} \quad & \frac{d}{ds} \int_0^\infty \rho V^2 \cos \theta \sin \sigma r dr = -\frac{F_D \cos^2 \theta \sin \sigma \cos \sigma}{2\pi \sqrt{1 - \cos^2 \theta \cos^2 \sigma}} && \text{(y-momentum)} \\
 \text{Eq. 22.} \quad & \frac{d}{ds} \int_0^\infty \rho V^2 \sin \theta r dr = \int_0^\infty (\rho_{amb} - \rho) g r dr - \frac{F_D \sin \theta \cos \theta \cos \sigma}{2\pi \sqrt{1 - \cos^2 \theta \cos^2 \sigma}} && \text{(z-momentum)} \\
 \text{Eq. 23.} \quad & \frac{d}{ds} \int_0^\infty \rho V Y r dr = 0 && \text{(species)} \\
 \text{Eq. 24.} \quad & \frac{d}{ds} \int_0^\infty \rho V h r dr = \frac{h_{amb} \rho_{amb} E}{2\pi} && \text{(energy)} \\
 \text{Eq. 25.} \quad & \frac{dx}{ds} = \cos \theta \cos \sigma && \text{(x-coordinate)} \\
 \text{Eq. 26.} \quad & \frac{dy}{ds} = \cos \theta \sin \sigma && \text{(y-coordinate)} \\
 \text{Eq. 27.} \quad & \frac{dz}{ds} = \sin \theta && \text{(z-coordinate)}
 \end{aligned}$$

Here E represents the turbulent air entrainment rate. The polar, θ , and azimuthal angles, σ , are used to specify the location of the stream wise coordinate, S . The impact of wind is accounted using the method by Jirka [51], where each segment treated as a uniform cylinder acted upon by a drag force, F_D , with a resulting pressure differential due to boundary layer separation on the downwind side. Accordingly, the velocity vector is aligned to the x -axis, and the transvers velocity component is given as a function of the wind speed, i.e., $U_w \sqrt{1 - \cos^2 \theta \cos^2 \sigma}$. The resulting drag force with an assumed cylinder diameter of $\sqrt{2}B$ is given by:

$$\text{Eq. 28.} \quad F_D = c_D \sqrt{2} B U_w \sqrt{1 - \cos^2 \theta \cos^2 \sigma}$$

Jirka empirically determined the drag coefficient, c_D , to be 1.3, which has not been validated for liquid hydrogen releases.

A number of investigators including most recently Houf and Schefer [46] have shown that within the Zone 4, the mean velocity profiles are nearly Gaussian and take the form:

$$\text{Eq. 29.} \quad V = V_{cl} \exp\left(-\frac{r^2}{B^2}\right)$$

Here the subscript “*cl*” denotes local centerline conditions and *B* is the characteristic jet half-width. Fay et al. [126] has shown that scalar profiles are Gaussian and can be expressed as:

$$\text{Eq. 30.} \quad \rho - \rho_{air} = (\rho_{cl} - \rho_{air}) \exp\left(-\frac{r^2}{\lambda^2 B^2}\right)$$

$$\text{Eq. 31.} \quad \rho Y = \rho_{cl} Y_{cl} \exp\left(-\frac{r^2}{\lambda^2 B^2}\right)$$

The relative velocity to scalar spreading ratio, λ , is related to the turbulent Prandtl and Schmidt numbers and a value of 1.16 works well for hydrogen. In these zones, it is assumed that hydrogen/air mixtures behave as calorically perfect ideal gas mixtures with constant component specific heats. The radial *h* profile can then be expressed as:

$$\text{Eq. 32.} \quad h = C_p T = \frac{C_p p_{amb} MW}{\rho R_u}$$

$$\text{Eq. 33.} \quad C_p = Y_{H_2} C_{p,H_2} + (1 - Y_{H_2}) C_{p,air}$$

$$\text{Eq. 34.} \quad MW = \left[\frac{Y_{H_2}}{MW_{H_2}} + \frac{1 - Y_{H_2}}{MW_{air}} \right]^{-1}$$

Here *MW* is the molecular weight and R_u is the ideal gas constant. The complicated radial distribution in *h* can be determined from Eq. 32 using Eqs. 30 and 31. Substitution of the radial velocity and state variable equations into the governing conservation equations (19-24) and integrating yields the following ordinary differential equations:

$$\text{Eq. 35.} \quad \frac{d}{ds} \left\{ V_{cl} B^2 \left[\rho_{amb} - \frac{\lambda^2}{\lambda^2 + 1} (\rho_{amb} - \rho_{cl}) \right] \right\} = \frac{\rho_{amb} E}{\pi}$$

$$\text{Eq. 36.} \quad \frac{d}{ds} \left\{ V_{cl}^2 B^2 \cos \theta \cos \sigma \left[\frac{\rho_{amb}}{2} - \frac{\lambda^2}{2\lambda^2 + 1} (\rho_{amb} - \rho_{cl}) \right] \right\} = \frac{F_D}{2\pi} \sqrt{1 - \cos^2 \theta \cos^2 \sigma}$$

$$\text{Eq. 37.} \quad \frac{d}{ds} \left\{ V_{cl}^2 B^2 \cos \theta \sin \sigma \left[\frac{\rho_{amb}}{2} - \frac{\lambda^2}{2\lambda^2 + 1} (\rho_{amb} - \rho_{cl}) \right] \right\} = -\frac{F_D \cos^2 \theta \sin \sigma \cos \sigma}{2\pi \sqrt{1 - \cos^2 \theta \cos^2 \sigma}} \quad (\text{y-mom.})$$

$$\text{Eq. 38.} \quad \frac{d}{ds} \left\{ V_{cl}^2 B^2 \sin \theta \left[\frac{\rho_{amb}}{2} - \frac{\lambda^2}{2\lambda^2 + 1} (\rho_{amb} - \rho_{cl}) \right] \right\} = (\rho_{amb} - \rho_{cl}) \lambda^2 B^2 - \frac{F_D \sin \theta \cos \theta \cos \sigma}{2\pi \sqrt{1 - \cos^2 \theta \cos^2 \sigma}}$$

$$\text{Eq. 39.} \quad \frac{d}{ds} \{ V_{cl} B^2 (\rho_{amb} Y_{amb} - \rho_{cl} Y_{cl}) \} = 0$$

$$\text{Eq. 40.} \quad \frac{d}{ds} \left\{ \int_0^\infty V \rho \left(h + \frac{1}{2} V^2 - h_{amb} \right) r dr \right\} = 0$$

Equations 25-27, and 35–40, represent a system of 9 ordinary differential equations with 9 unknowns (*x*, *y*, *z*, θ , σ , *B*, ρ_{cl} , V_{cl} , and Y_{cl}). Commercial differential- solvers (e.g., ODE45 from Matlab) can simultaneously solve these equations. The energy conservation equation integral in the Eq. 40 must be numerically solved, with convergence achieved with an upper integration limit of 3*B* discretized into 1000 equally spaced intervals and the use of the Trapezoid rule.

A model for Zone 3, the zone of flow establishment, was used to compute the initial values of the dependent variables (e.g. initial centerline values for density, velocity, mass fraction, enthalpy, etc.) at Station 4. Detailed documentation is provided in reference [69].

To close the system of equations, a model for the entrainment in Eq. 35 is needed. In the absence of data for air entrainment into cold hydrogen jets, the entrainment model of Houf and Schefer [46] is used, which is based on an approach suggested by Hirst [127]. References [46, 69] contain a detailed description of the entrainment model.

3 Proposed Experimental Approach to Model Validation

Experimental data from well-controlled cryogenic hydrogen releases are needed to validate existing CFD simulation approaches and improve the performance of the reduced-order dispersion models described in Section 2. To the best of the authors' knowledge, no test-facility currently exists that can produce relevant flow rates of accurately metered compressed hydrogen releases at or near the saturation condition into an ambient environment unperturbed by spurious currents. Moreover, particularly relevant experiments would have controlled ambient humidity levels in the surrounding air. The proposed facility to address these needs is shown schematically in Figure 3. It includes a novel delivery system designed to cool gaseous hydrogen to temperatures near or even below the condensation point. These cryogenic gas and mixed-phase flows will be released into the ambient test-section through a specially designed cryogenic nozzle within the Sandia/CA Cryogenic Hydrogen Release Laboratory. Jet properties will be characterized using advanced imaging diagnostics such as planar laser Rayleigh scatter, capable of accurate instantaneous hydrogen concentration measurements, and particle image velocimetry used for complementary flow velocity measurements.

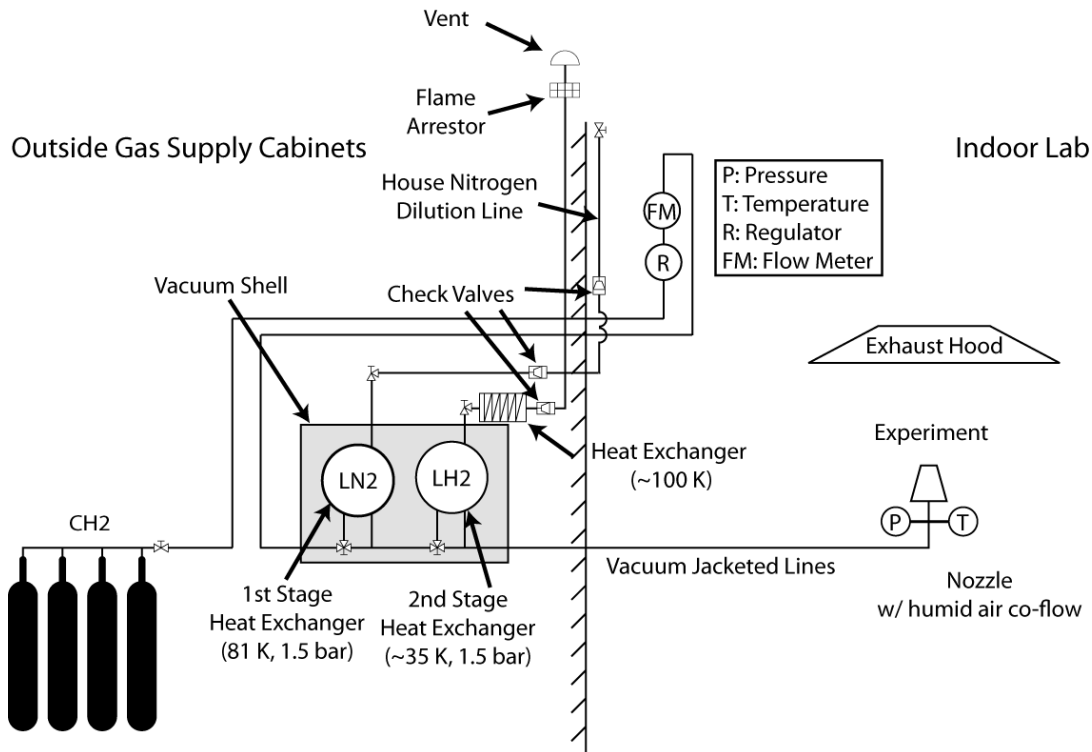


Figure 3. Schematic layout of the proposed Sandia/CA Cryogenic Hydrogen Release Laboratory that illustrates the two-stage heat-exchanger (liquid nitrogen and liquid hydrogen) to rapidly cool supplied gaseous hydrogen to the desired cryogenic temperature at the nozzle exit.

The crucial modification to the current Turbulent Combustion Laboratory is the integration of a dual-stage heat-exchanger assembly into the existing gas supply system. For the proposed system, ambient temperature compressed hydrogen will flow into the lab where it will be

metered and regulated to the desired downstream pressure and flow rate via an existing Tescom flow meter, which has been successfully used previously to produce controlled flow rates for compressed hydrogen release jets [50, 67]. The flow will then be directed into the dual-stage heat exchanger assembly that will be housed outside in a vacuum insulated shell casing to minimize heat leak to the coolant gas. The first stage heat-exchanger will contain liquid nitrogen held at 1.5 bar absolute that surrounds a large network of coiled tubing through which the compressed hydrogen will flow. Heat transfer from the warmer gas-phase hydrogen to the cooler liquid nitrogen will result in a steady boil-off of the coolant liquid, with the resulting saturated gas vented by a pressure relief device into the lab’s exhaust hood. The length of tubing within the heat exchanger will be sufficient to reduce the exit hydrogen gas temperature to the nitrogen saturation temperature (~81 K at 1.5 bar).

The hydrogen flow will then be directed into a second stage heat exchanger that uses liquid hydrogen, again held at 1.5 bar, to cool the incoming hydrogen flow to the desired temperature based on the internal tubing length and the gas flow rates. Since the hydrogen coolant is very cold at saturation conditions (~31.4 K at 1.5 bar), it will be necessary to run the coolant gas through an external heat exchanger before it is released into the ambient, to prevent the formation of an ice plug due to frozen air constituents. Moreover, since hydrogen is flammable, it will be necessary to dilute the downstream vent gas using a combination of house nitrogen and vent gas from the first stage cooler. Check valves will be used to prevent vent gas back-flows.

Two alternate coolant fluids with sufficiently low condensation points that could be used in lieu of hydrogen to eliminate the need for a flammable coolant gas are helium and neon. However, neon can be rejected immediately since the available supply in the quantities needed for a single test (~10s of kilograms) is not available. Helium is (slightly) more readily available; however, low heats of vaporization relative to hydrogen make it a poor coolant gas. For example, the amount of liquid hydrogen or liquid helium required for the second stage heat-exchanger are detailed in Table 1 for 3 flow rates of hydrogen at 10 bar to produce the same hydrogen exit temperature. From this table, it is apparent that an order of magnitude additional liquid helium coolant is required to reach the same hydrogen exit flow temperature. Procurement and storage of such large helium quantities is prohibitive.

Table 1. Amount of liquid nitrogen coolant required for the 1st stage heat-exchanger and either liquid hydrogen or liquid helium coolant required for the 2nd stage heat-exchanger hydrogen flow rates between 100 and 1000 SLPM. The hydrogen inflows are at 10 bar atmospheric, and the exit temperature are either 35 K (cold vapor) or 31.3 K saturated liquid.

Temperature [K]	H ₂ Flow Rate [SLPM]	LN ₂ [lit] 1 st Stage	LH ₂ [lit] 2 nd Stage	LHe [lit] 2 nd Stage
Cold Hydrogen Gas				
35	100	10.2	10.7	165.7
35	500	51.2	53.6	828.7
35	1000	102.4	107.2	1657.3
Saturated Liquid Hydrogen				
31.3	100	10.2	16.9	260.6
31.3	500	51.2	84.3	1302.8
31.3	1000	102.4	168.5	2605.5

Once the hydrogen flows are cooled to the desired temperatures, they will flow in vacuum jacked lines until they reach the exit nozzle, where pressure and temperature will be monitored at the exit point. Note that a small co-flow will be used to limit the influence of spurious room currents (e.g., from the climate control system) onto jet dynamics. Note further that the amount of ambient humidity will be actively controlled in the co-flow air, either through the use of an upstream water boiler and heat-exchanger assembly, or through the use of bottled air with certified humidity levels.

4 Summary and Recommendations

Hydrogen refueling infrastructure is needed as consumers purchase FCEVs, a need that is recognized and supported by the DOE's EERE FCTO. Past support from the FCTO has led to defensible, risk-informed fire safety codes for siting compressed gas refueling stations. The higher return on investment from liquid hydrogen storage systems due to higher potential system throughput makes these systems more desirable. However, the current separation distances in the fire safety codes are based largely on subjective expert opinion that constrains station design in congested marketplaces. This work summarizes the current understanding of cryogenic hydrogen releases and outlines a path forward to develop defensible, risk-informed fire safety codes for liquid hydrogen, analogous to the compressed gas codes.

Reduced-order models that can be used to efficiently span a wide scenario space are essential to support physics-informed QRA toolkits used to develop risk-informed fire safety codes. A reduced-order model for dispersion from liquid hydrogen sources, COLDPLUME, is presented in this work, but this model lacks adequate validation data. The available data in the literature for cryogenic hydrogen releases is comprised of four experimental campaigns, most with poor control of the boundary conditions and sparse measurements of relevant data (e.g. hydrogen concentration). The level of agreement between CFD models and these experiments is decent (often within a factor of 2), but it is unclear whether the discrepancies arise due to inaccurate model physics or the poor experimental boundary condition control. It is impractical to use this data to validate COLDPLUME or other reduced-order models, or to use CFD simulations to develop reduced-order models, as they have not been sufficiently validated themselves.

Release and hazard models that have been developed for compressed hydrogen sources provide a good starting point to modeling releases and hazards from cryogenic hydrogen sources, but several physical differences that need to be addressed have been identified in this work. Specific challenges include thermodynamic state and phase change modeling for cold hydrogen flows and flows of multi-phase mixtures which may be comprised of solids (moisture and air may condense), liquids, non-ideal gases, and supercritical fluids. Reduced-order models also need to describe the dynamics of surface impingement, to capture interactions with the ground, and if barrier walls will be used to mitigate release hazards, as they are for gaseous releases.

The experiment proposed in this work will begin to address the lack of validation data for cryogenic hydrogen releases. A dual-stage heat-exchanger assembly will be incorporated into the existing gas supply system of the Turbulent Combustion Laboratory, and high-fidelity diagnostics will be applied to releases of cold and potentially multi-phase hydrogen. The boundary conditions in this lab-scale setting will be well-characterized, including the humidity levels of the air entrained into the jet. This data will be used for further development and validation of the COLDPLUME model.

References

- [1] Brown T, Schell LS, Stephens-Romero S, Samuelson S, Economic analysis of near-term California hydrogen infrastructure. *Int J Hydrogen Energy*, 2013;38:3846-57.
- [2] Harris AP, Benchmarks and supporting details for US DOE FCTO SCS subprogram metrics Livermore, CA: SAND-XXXX, Sandia National Laboratories, 2014.
- [3] Hydrogen Technologies Code, National Fire Protection Agency, NFPA 2, Quincy, MA, 2011.
- [4] Hart N, Gaseous Hydrogen Refuelling Stations - DSEAR hazardous areas and separation distances. Thesis, University of Ulster; 2014.
- [5] LaChance J, Houf W, Middleton B, Fluer L, Analyses to Support Development of Risk-Informed Separation Distances for Hydrogen Codes and Standards. SAND 2009-0874, Sandia National Laboratories, March, 2009.
- [6] Schefer RW, Groethe M, Houf WG, Evans G, Experimental evaluation of barrier walls for risk reduction of unintended hydrogen releases. *Int J Hydrogen Energy*, 2009;34:1590-606.
- [7] Boon-Brett L, Bousek J, Castello P, Salyk O, Harskamp F, Aldea L, et al., Reliability of commercially available hydrogen sensors for detection of hydrogen at critical concentrations: Part I - Testing facility and methodologies. *Int J Hydrogen Energy*, 2008;33:7648-57.
- [8] Boon-Brett L, Bousek J, Moretto P, Reliability of commercially available hydrogen sensors for detection of hydrogen at critical concentrations: Part II - selected sensor test results. *Int J Hydrogen Energy*, 2009;34:562-71.
- [9] Buttner WC, Post MP, Burgess R, Rivkin C, An overview of hydrogen safety sensors and requirements. *Int J Hydrogen Energy*, 2010;in press.
- [10] Custer RLP, Meacham BJ, "SFPE Engineering Guide to Performance-Based Fire Protection." Quincy, MA: National Fire Protection Association, 2007.
- [11] Groth K, Harris A, Hydrogen Quantitative Risk Assessment Workshop Proceedings. SAND2013-7888, Sandia National Laboratories, 2013.
- [12] Groth KM, Tchouvelev AV, A toolkit for integrated deterministic and probabilistic risk assessment for hydrogen infrastructure. Proc International Conference on Probabilistic Safety Assessment and Management (PSAM 12), 2014.

- [13] Tchouvelev AV, Groth KM, Benard P, Jordan T, A Hazard Assessment Toolkit For Hydrogen Applications. Proc 20th World Hydrogen Energy Conference (WHEC 2014), 2014.
- [14] Kotchourko A, Baraldi D, Benard P, Eisenreich N, Jordan T, Keller J, et al., State of the art and research priorities in hydrogen safety. Proc European Joint Research Centre, 2014.
- [15] Rose S, Flamberg S, Levernz F, Guidance Document for Incorporating Risk Concepts into NFPA Codes and Standards. Quincy, MA: NFPA, http://www.nfpa.org/~media/Files/Research/Research%20Foundation/risk-based_codes_and_stds.pdf, 2007.
- [16] LaChance J, Tchouvelev A, Engebo A, Development of uniform harm criteria for use in quantitative risk analysis of the hydrogen infrastructure. Int J Hydrogen Energy, 2011;36:59-66.
- [17] Groth KM, LaChance JL, Harris AP, Early-Stage Quantitative Risk Assessment to Support Development of Codes and Standard Requirements for Indoor Fueling of Hydrogen Vehicles. SAND2012-10150, Sandia National Laboratories, 2012.
- [18] Weiner SC, Fassbender LL, Blake C, Aceves SM, Somerday BP, Ruiz A, Web-based resources enhance hydrogen safety knowledge. Int J Hydrogen Energy, 2013;38:7583-93.
- [19] Cristina Galassi M, Papanikolaou E, Baraldi D, Funnemark E, Håland E, Engebø A, et al., HIAD – hydrogen incident and accident database. Int J Hydrogen Energy, 2012;37:17351-7.
- [20] Groth KM, LaChance JL, Harris AP, Design-stage QRA for indoor vehicular hydrogen fueling systems. Proc European Society for Reliability Annual Meeting (ESREL), 2013.
- [21] Hankinson G, Lowesmith BJ, A consideration of methods of determining the radiative characteristics of jet fires. Combust Flame, 2012;159:1165-77.
- [22] Miller D, Jung S, Lutostansky E, Applicability of currently available flare radiation models for hydrogen and syngas. Process Saf Prog, 2014:n/a-n/a.
- [23] Ekoto IW, Houf WG, Ruggles AJ, Creitz LW, Li JX, Large-Scale Hydrogen Jet Flame Radiant Fraction Measurements and Modeling. Proc International Pipeline Conference, Calgary, Canada, Sept 24-28, 2012.
- [24] Kotchourko A, Baraldi D, Benard P, Jordan T, Kessler A, LaChance J, et al., State-of-the-Art and Research Priorities in Hydrogen Safety. Proc 5th International Conference on Hydrogen Safety, Brussels, Belgium, Sept 9-11, 2013.
- [25] Pritchard DK, Rattigan WM, Hazards of liquid hydrogen. Buxton, Derbyshire, UK: Health and Safety Laboratory, 2010.

- [26] Witcofski RD, Chirivella JE, Experimental and Analytical Analyses of the Mechanisms Governing the Dispersion of Flammable Clouds Formed by Liquid-Hydrogen Spills. *Int J Hydrogen Energy*, 1984;9:425-35.
- [27] Chirivella JE, Witcofsk RD, Experimental results from fast 1500 gallon LH2 spills. *Proc American Institute of Chemical Engineers Symposium*, 251, 1986, p. 120-40.
- [28] Schmidtchen U, Marinescupasoi L, Verfondern K, Nickel V, Sturm B, Dienhart B, Simulation of Accidental Spills of Cryogenic Hydrogen in a Residential Area. *Cryogenics*, 1994;34:401-4.
- [29] Verfondern K, Dienhart B, Experimental and theoretical investigation of liquid hydrogen pool spreading and vaporization. *Int J Hydrogen Energy*, 1997;22:649-60.
- [30] Verfondern K, Dienhart B, Pool spreading and vaporization of liquid hydrogen. *Int J Hydrogen Energy*, 2007;32:2106-17.
- [31] Nakamichi K, Kihara Y, Okamura T, Observation of liquid hydrogen jet on flashing and evaporation characteristics. *Cryogenics*, 2008;48:26-30.
- [32] Proust C, Lacombe JM, Jamois D, Perrette L, Process of the formation of large unconfined clouds following a massive spillage of liquid hydrogen on the ground. *Proc 2nd International Conference on Hydrogen Safety, San Sebastian, Spain, Sept 11-13, 2007*.
- [33] Hooker P, Willoughby DB, Experimental releases of liquid hydrogen. *Proc 4th International Conference on Hydrogen Safety, San Francisco, CA, USA, Sept 12 - 14, 2011*.
- [34] Royle M, Willoughby D, The safety of the future hydrogen economy. *Process Saf Environ*, 2011;89:452-62.
- [35] Friedrich A, Breitung W, Stern G, Vesper A, Kuznetsov M, Fast G, et al., Ignition and heat radiation of cryogenic hydrogen jets. *Int J Hydrogen Energy*, 2012;37:17589-98.
- [36] Sklavounos S, Rigas F, Fuel gas dispersion under cryogenic release conditions. *Energy Fuel*, 2005;19:2535-44.
- [37] Middha P, Ichard M, Arntzen BJ, Validation of CFD modelling of LH2 spread and evaporation against large-scale spill experiments. *Int J Hydrogen Energy*, 2011;36:2620-7.
- [38] Venetsanos AG, Bartzis JG, CFD modeling of large-scale LH2 spills in open environment. *Int J Hydrogen Energy*, 2007;32:2171-7.
- [39] Baraldi D, Venetsanos AG, Papanikolaou E, Heitsch M, Dallas V, Numerical analysis of release, dispersion and combustion of liquid hydrogen in a mock-up hydrogen refuelling station. *J Loss Prevent Proc*, 2009;22:303-15.

- [40] Schmidt D, Krause U, Schmidtchen U, Numerical simulation of hydrogen gas releases between buildings. *Int J Hydrogen Energy*, 1999;24:479-88.
- [41] Statharas JC, Venetsanos AG, Bartzis JG, Wurtz J, Schmidtchen U, Analysis of data from spilling experiments performed with liquid hydrogen. *J Hazard Mater*, 2000;77:57-75.
- [42] Ichard M, Hansen OR, Middha P, Willoughby D, CFD computations of liquid hydrogen releases. *Int J Hydrogen Energy*, 2012;37:17380-9.
- [43] Jaekel C, Verfondern K, Kelm S, Jahn W, Allelein HJ, 3D Modeling of the different boiling regimes during spill and spreading of liquid hydrogen. *Enrgy Proced*, 2012;29:244-53.
- [44] Giannissi SG, Venetsanos AG, Markatos N, Willoughby DB, Royle M, Simulation of Hydrogen Dispersion Under Cryogenic Release Conditions. *Proc nternational Conference on Hydrogen Safety 5*, Brussels, Belgium, 2013.
- [45] Winters WS, A New Approach to Modeling Fluid/Gas Flows in Networks. SAND2001-8422, Sandia National Laboratories, July, 2001.
- [46] Houf W, Schefer R, Analytical and experimental investigation of small-scale unintended releases of hydrogen. *Int J Hydrogen Energy*, 2008;33:1435-44.
- [47] Schefer RW, Houf WG, San Marchi C, Chernicoff WP, Englom L, Characterization of leaks from compressed hydrogen dispensing systems and related components. *Int J Hydrogen Energy*, 2006;31:1247-60.
- [48] Schefer RW, Houf WG, Williams TC, Investigation of small-scale unintended releases of hydrogen: momentum-dominated regime. *Int J Hydrogen Energy*, 2008;33:6373-84.
- [49] Schefer RW, Houf WG, Williams TC, Investigation of small-scale unintended releases of hydrogen: Buoyancy effects. *Int J Hydrogen Energy*, 2008;33:4702-12.
- [50] Ruggles AJ, Ekoto IW, Ignitability and mixing of underexpanded hydrogen jets. *Int J Hydrogen Energy*, 2012;37:17549-60.
- [51] Jirka GH, Integral model for turbulent buoyant jets in unbounded stratified flows. Part I: Single round jet. *Environ Fluid Mech*, 2004;4:1-56.
- [52] Laneserff GF, Linden PF, Hillel M, Forced, Angled Plumes. *J Hazard Mater*, 1993;33:75-99.
- [53] Xiao JJ, Travis JR, Breitung W, Non-Boussinesq Integral Model for Horizontal Turbulent Strongly Buoyant Plane Jets. *Icone16: Proceeding of the 16th International Conference on Nuclear Engineering - 2008, Vol 3*, 2008:225-32.

- [54] Epstein M, Fauske HK, Total flammable mass and volume within a vapor cloud produced. by a continuous fuel-gas or volatile liquid-fuel release. *J Hazard Mater*, 2007;147:1037-50.
- [55] Beck SBM, Bagshaw NM, Yates JR, Explicit equations for leak rates through narrow cracks. *Int J Pres Ves Pip*, 2005;82:565-70.
- [56] Birch AD, Brown DR, Dodson MG, Swaffield F, The Structure and Concentration Decay of High-Pressure Jets of Natural-Gas. *Combust Sci Technol*, 1984;36:249-61.
- [57] Ewan BCR, Moodie K, Structure and Velocity-Measurements in Underexpanded Jets. *Combust Sci Technol*, 1986;45:275-88.
- [58] Molkov VV, Makarov DV, Bragin MV, Physics and modelling of underexpanded jets and hydrogen dispersion in atmosphere. *Proc 24th International Conference on Interaction of Intense Energy Fluxes with Matter, Elbrus, Mar 1-6, 2009*.
- [59] Schefer RW, Houf WG, Williams TC, Bourne B, Colton J, Characterization of high-pressure, underexpanded hydrogen-jet flames. *Int J Hydrogen Energy*, 2007;32:2081-93.
- [60] Birch AD, Hughes DJ, Swaffield F, Velocity Decay of High-Pressure Jets. *Combust Sci Technol*, 1987;52:161-71.
- [61] Yüceil KB, Ötügen MV, Scaling parameters for underexpanded supersonic jets. *Phys Fluids*, 2002;14:4206-15.
- [62] Harstad K, Bellan J, Global analysis and parametric dependencies for potential unintended hydrogen-fuel releases. *Combust Flame*, 2006;144:89-102.
- [63] Papanikolaou E, Baraldi D, Kuznetsov M, Venetsanos A, Evaluation of notional nozzle approaches for CFD simulations of free-shear under-expanded hydrogen jets. *Int J Hydrogen Energy*, 2012;37:18563-74.
- [64] Menon N, Skews BW, Shock wave configurations and flow structures in non-axisymmetric underexpanded sonic jets. *Shock Waves*, 2010;20:175-90.
- [65] Shishehgaran N, Paraschivoiu M, CFD based simulation of hydrogen release through elliptical orifices. *Int J Hydrogen Energy*.
- [66] Rajakuperan E, Ramaswamy MA, An experimental investigation of underexpanded jets from oval sonic nozzles. *Exp Fluids*, 1998;24:291-9.
- [67] Ruggles AJ, Ekoto IW, Experimental Investigation of Nozzle Aspect Ratio Effects on Underexpanded Hydrogen Jet Release Characteristics. *Proc International Conference on Hydrogen Safety 5, Brussels, Belgium, 2013*.

- [68] Makarov D, Molkov V, Structure and Concentration Decay in Supercritical Plane Hydrogen Jet. Proc Eight International Symposium on Hazards, Prevention, and Mitigation of Industrial Explosions, Yokohama, Japan, ISH073, September 5-10, 2010.
- [69] Winters WS, Modeling Leaks from Liquid Hydrogen Storage Systems. SAND Report 2009-0035, Sandia National Laboratories, 2009.
- [70] Winters WS, Houf WG, Simulation of small-scale releases from liquid hydrogen storage systems. Int J Hydrogen Energy, 2011;36:3913-21.
- [71] Houf WG, Winters WS, Simulation of high-pressure liquid hydrogen releases. Int J Hydrogen Energy, 2013;38:8092-9.
- [72] Travis JR, Koch DP, Breitung W, A homogeneous non-equilibrium two-phase critical flow model. Int J Hydrogen Energy, 2012;37:17373-9.
- [73] Simoneau RJ, Hendricks RC, Two-phase choked flow of cryogenic fluids in converging-diverging nozzles. Technical Paper 1484, NASA, 1979.
- [74] Hendricks RC, Simoneau RJ, Barrows RF, Two-phase choked flow of subcooled oxygen and nitrogen. Technical Note TN-8169, NASA, 1976.
- [75] Li ZY, Pan XM, Meng X, Ma JX, Study on the harm effects of releases from liquid hydrogen tank by consequence modeling. Int J Hydrogen Energy, 2012;37:17624-9.
- [76] Li Z, Pan X, Sun K, Ma J, Comparison of the harm effects of accidental releases: Cryo-compressed hydrogen versus natural gas. Int J Hydrogen Energy, 2013;38:11174-80.
- [77] Kim M, Do K, Choi B, Han Y, First-order perturbation solutions of liquid pool spreading with vaporization. Int J Hydrogen Energy, 2011;36:3268-71.
- [78] Kim M, Do K, Choi B, Han Y, High-order perturbation solutions to a LH2 spreading model with continuous spill. Int J Hydrogen Energy, 2012;37:17409-14.
- [79] Cleaver RP, Marshall MR, Linden PF, The Buildup of Concentration within a Single Enclosed Volume Following a Release of Natural-Gas. J Hazard Mater, 1994;36:209-26.
- [80] Lowesmith BJ, Hankinson G, Spataru C, Stobbart M, Gas build-up in a domestic property following releases of methane/hydrogen mixtures. Int J Hydrogen Energy, 2009;34:5932-9.
- [81] Ivings MJ, Lea CJ, Webber DM, Jagger SF, Coldrick S, A protocol for the evaluation of LNG vapour dispersion models. J Loss Prevent Proc, 2013;26:153-63.
- [82] Cariteau B, Brinster J, Tkatschenko I, Experiments on the distribution of concentration due to buoyant gas low flow rate release in an enclosure. Int J Hydrogen Energy, 2011;36:2505-12.

- [83] Ekoto IW, Houf WG, Evans GH, Merilo EG, Groethe MA, Experimental investigation of hydrogen release and ignition from fuel cell powered forklifts in enclosed spaces. *Int J Hydrogen Energy*, 2012;37:17446-56.
- [84] Kaye NB, Hunt GR, Time-dependent flows in an emptying filling box. *J Fluid Mech*, 2004;520:135-56.
- [85] Worster MG, Huppert HE, Time-Dependent Density Profiles in a Filling Box. *J Fluid Mech*, 1983;132:457-66.
- [86] Tang MJ, Baker QA, A new set of blast curves from vapor cloud explosions. *Proc 33rd AIChE Loss Prevention Symposium*, Houston, TX, Mar 14-18, 1999.
- [87] Sari A, Comparison of TNO Multienergy and Baker-Strehlow-Tang Models. *Process Saf Prog*, 2011;30:23-6.
- [88] Gostintsev YA, Istratov AG, Shulenin YV, Self-Similar Propagation of a Free Turbulent Flame in Mixed Gas-Mixtures. *Combust Explo Shock+*, 1988;24:563-9.
- [89] Tomizuka T, Kuwana K, Mogi T, Dobashi R, Koshi M, A study of numerical hazard prediction method of gas explosion. *Int J Hydrogen Energy*, 2013;38:5176-80.
- [90] Park DJ, Lee YS, A comparison on predictive models of gas explosions. *Korean J Chem Eng*, 2009;26:313-23.
- [91] AIChE, Guidelines for Evaluating the Characteristics of Vapor Cloud Explosions, Flash Fires, and BLEVEs. New York: American Institute of Chemical Engineers, 1994.
- [92] Baker QA, Tang MJ, Scheler EA, Silva GJ, Vapor cloud explosion analysis. *Process Saf Prog*, 1996;15:106-9.
- [93] Tamanini F, Dust explosion vent sizing - Current methods and future developments. *J Phys Iv*, 2002;12:31-44.
- [94] Bauwens CR, Chaffee J, Dorofeev S, Effect of Ignition Location, Vent Size, and Obstacles on Vented Explosion Overpressures in Propane-Air Mixtures. *Combust Sci Technol*, 2010;182:1915-32.
- [95] Bauwens CR, Chaffee J, Dorofeev SB, Vented explosion overpressures from combustion of hydrogen and hydrocarbon mixtures. *Int J Hydrogen Energy*, 2011;36:2329-36.
- [96] Bauwens CR, Chao J, Dorofeev SB, Effect of hydrogen concentration on vented explosion overpressures from lean hydrogen-air deflagrations. *Int J Hydrogen Energy*, 2012;37:17599-605.
- [97] Brennan S, Molkov V, Safety assessment of unignited hydrogen discharge from onboard storage in garages with low levels of natural ventilation. *Int J Hydrogen Energy*, 2013;38:8159-66.

- [98] Bauwens CR, Dorofeev SB, CFD modeling and consequence analysis of an accidental hydrogen release in a large scale facility. *Int J Hydrogen Energy*.
- [99] Groth KM, Hydrogen behavior and Quantitative Risk Assessment. *Proc Annual Merrit Review*, Washington D.C., 2014.
- [100] Birch AD, Brown DR, Dodson MG, Ignition probabilities in turbulent mixing flows. *P Combust Inst*, 1981;18:1775-80.
- [101] Birch AD, Brown DR, G. DM, Thomas JR, Studies of Flammability in Turbulent Flows using Laser Raman Spectroscopy. *P Combust Inst*, 1979;17:307-14.
- [102] Birch AD, Brown DR, Cook DK, Hargrave GK, Flame Stability in Underexpanded Natural-Gas Jets. *Combust Sci Technol*, 1988;58:267-80.
- [103] Schefer RW, Evans GH, Zhang J, Ruggles AJ, Greif R, Ignitability limits for combustion of unintended hydrogen releases: Experimental and theoretical results. *Int J Hydrogen Energy*, 2011;36:2426-35.
- [104] Chamberlain GA, Developments in Design Methods for Predicting Thermal-Radiation from Flares. *Chem Eng Res Des*, 1987;65:299-309.
- [105] Cook DK, Fairweather M, Hammonds J, Hughes DJ, Size and Radiative Characteristics of Natural-Gas Flares .1. Field Scale Experiments. *Chem Eng Res Des*, 1987;65:310-7.
- [106] Sivathanu YR, Gore JP, Total Radiative Heat-Loss in Jet Flames from Single-Point Radiative Flux Measurements. *Combust Flame*, 1993;94:265-70.
- [107] Johnson AD, Brightwell HM, Carsley AJ, A Model for Predicting the Thermal-Radiation Hazards from Large-Scale Horizontally Released Natural-Gas Jet Fires. *Process Saf Environ*, 1994;72:157-66.
- [108] Guide for Pressure-Relieving and Depressuring Systems, 4th edition, American Petroleum Institute, API 521, 1997.
- [109] Shrivill LC, Roberts P, Butler CJ, Roberts TA, Royle M, Characterisation of the hazards from jet releases of hydrogen. *Proc 1st International Conference on Hydrogen Safety*, Pisa, Italy, Sept 8-10, 2005.
- [110] Lowesmith BJ, Hankinson G, Acton MR, Chamberlain G, An overview of the nature of hydrocarbon jet fire hazards in the oil and gas industry and a simplified approach to assessing the hazards. *Process Saf Environ*, 2007;85:207-20.
- [111] Houf W, Schefer R, Predicting radiative heat fluxes and flammability envelopes from unintended releases of hydrogen. *Int J Hydrogen Energy*, 2007;32:136-51.
- [112] Turns SR, Myhr FH, Oxides of Nitrogen Emissions from Turbulent Jet Flames - .1. Fuel Effects and Flame Radiation. *Combust Flame*, 1991;87:319-35.

- [113] Molina A, Schefer RW, Houf WG, Radiative fraction and optical thickness in large-scale hydrogen-jet fires. *P Combust Inst*, 2007;31:2565-72.
- [114] Ekoto IW, Ruggles AJ, Li X, Creitz LW, Updated Jet Flame Radiation Modeling with Corrections for Buoyancy. *Proc International Conference on Hydrogen Safety 5*, Brussels, Belgium, 2013.
- [115] Azim MA, On the Structure of a Plane Turbulent Wall Jet. *J Fluid Eng-T Asme*, 2013;135.
- [116] Barenblatt GI, Chorin AJ, Prostokishin VM, The turbulent wall jet: A triple-layered structure and incomplete similarity. *P Natl Acad Sci USA*, 2005;102:8850-3.
- [117] George WK, Abrahamsson H, Eriksson J, Karlsson RI, Lofdahl L, Wosnik M, A similarity theory for the turbulent plane wall jet without external stream. *J Fluid Mech*, 2000;425:367-411.
- [118] Schwarz WH, Cosart WP, The 2-Dimensional Turbulent Wall-Jet. *J Fluid Mech*, 1961;10:481-95.
- [119] Lemmon EW, Huber ML, MO M, NIST reference fluid thermodynamic and transport properties-REFPROP. Gaithersburg, MD: U. S. Department of Commerce Technology Administration, National Institute of Standards and Technology, Standard Reference Data Program, April, 2007.
- [120] Moody FJ, Maximum Flow Rate of a Single Component 2-Phase Mixture. *J Heat Transf*, 1965;87:134-&.
- [121] Henry RE, Fauske HK, 2-Phase Critical Flow of One-Component Mixtures in Nozzles, Orifices, and Short Tubes. *J Heat Transf*, 1971;93:179-&.
- [122] Jeong JJ, Ha KS, Chung BD, Lee WJ, Development of a multi-dimensional thermal-hydraulic system code, MARS 1.3.1. *Ann Nucl Energy*, 1999;26:1611-42.
- [123] Chung MS, Park SB, Lee HK, Sound speed criterion for two-phase critical flow. *J Sound Vib*, 2004;276:13-26.
- [124] Crist S, Sherman PM, Glass DR, Study of Highly Underexpanded Sonic Jet. *Aiaa J*, 1966;4:68-&.
- [125] Gebhart B, Hilder DS, Kelleher M, "The diffusion of turbulent buoyant jets." Orlando, FL: Academic Press, Inc., 1984.
- [126] Fay JA, Escudier MP, Hoult DP, Halliday EC, Briggs GA, Bringfel.B, Discussions of Plume Rise Measurements at Industrial Chimneys. *Atmos Environ*, 1969;3:311-&.
- [127] Hirst EA, Analysis of buoyant jets within the zone of flow establishment. Report ORNL-TM-3470, Oak Ridge National Laboratory, 1971.

Distribution

1. Charles (Will) James Jr, PhD
U.S. Department of Energy
Office of Energy Efficiency & Renewable Energy
Fuel Cell Technologies Office
Safety, Codes, and Standards
1000 Independence Avenue, SW
Washington, DC 20585
2. Nitin Natesan
Linde LLC
2389 Lincoln Avenue, Hayward, CA 94545
Hayward, CA
3. Mike Ciotti
Linde LLC
575 Mountain Avenue
Murray Hill, NJ 07974
4. Aaron Harris
Air Liquide Corporation
2700 Post Oak Blvd.
Houston, TX 77056
5. MS0748 A. Christine LaFleur 6231
6. MS0748 Katrina M. Groth 6231
7. MS0784 Mitch McCrory 6231
8. MS0748 Katrina Groth 6231
9. MS9161 Chris San Marchi 8252
10. MS9052 Isaac W. Ekoto 8367
11. MS9052 Ethan Hecht 8367
12. MS9052 Daniel E. Dedrick 8367
13. MS9054 Robert Q. Hwang 8300
14. MS9054 Arthur E. Pontau 8360
15. MS0899 Technical Library 9536 (electronic copy)
16. MS0115 OFA/NFE Agreements 10012

